Journal of Cell Science 109, 499-508 (1996)
Printed in Great Britain © The Company of Biologists Limited 1996
JCS3316

Altered aggrecan synthesis correlates with cell and nucleus structure in statically compressed cartilage

Michael D. Buschmann[1,2,*], Ernst B. Hunziker[1], Young-Jo Kim[3] and Alan J. Grodzinsky[3]

[1]M. E. Mueller Institute for Biomechanics, University of Bern, Bern, Switzerland
[2]Biomedical Engineering Institute, Ecole Polytechnique of Montreal and Faculty of Medicine, University of Montreal, PO Box 6079 Station Centre-Ville, Montreal, Quebec, Canada, H3C 3A7
[3]Department of Electrical Engineering and Computer Science, Massachusetts Institute of Technology, Cambridge, MA, USA

*Author for correspondence at address 2 (e-mail: mike@grbb.polymtl.ca)

SUMMARY

Previous studies have shown that static equilibrium compression of cartilage tissue in vivo and in vitro decreases chondrocyte synthesis of aggrecan molecules. In order to identify mechanisms of cellular response to loading, we have investigated alterations in cell and nucleus structure and the accompanying changes in the synthesis of aggrecan in statically compressed cartilage explants. Using glutaraldehyde fixation and quantitative autoradiography of compressed and radiolabeled cartilage disks we spatially localized newly synthesized aggrecan. Using stereological tools to analyze these same specimens we estimated the cell and nucleus volume, surface area and directional radii. We found that aggrecan synthesis was reduced overall in compressed tissue disks. However, the compression induced a spatial (radial) inhomogeneity in aggrecan synthesis which was not present in uncompressed disks. This spatial inhomogeneity appeared to be directly related to mechanical boundary conditions and the manner in which the load was applied and, therefore, may represent a spatially specific functional adaptation to mechanical loading. Coincident with reduced aggrecan synthesis, we observed reductions in cell and nucleus volume and radii in the direction of compression which were in approximate proportion to the reduction in tissue thickness. Cell and nucleus dimensions perpendicular to the direction of compression did not change significantly. Therefore the observed deformation of the cell and nucleus in statically compressed cartilage approximately followed the dimensional changes imposed on external specimen surfaces. The strong correlation observed between local changes in aggrecan synthesis and alterations in cell and nucleus structure also lend support to certain hypotheses regarding the intracellular signal transduction pathways that may be important in the biosynthetic response of chondrocytes to mechanical loading.

Key words: Biomechanics, Stress (mechanical), Autoradiography, Proteoglycan, Aggrecan, Cartilage, Chondrocyte

INTRODUCTION

Articular cartilage forms the articulating surfaces in diarthroidal joints. With synovial fluid, it endows a joint with low-friction surfaces and in conjunction with ligaments, tendons and menisci, transmits and distributes forces to the underlying bone. The biomechanical properties of articular cartilage result from a complex interaction of genetic and environmental factors during development and growth leading to a heterogeneous, anisotropic material composed of chondrocytes, which occupy 1-10% of tissue volume, and an extracellular matrix (ECM) of high (~70%) water content. Characterization of its mechanical properties have shown a highly viscoelastic behavior (Mow et al., 1984), coupled to electromechanical phenomena (Frank and Grodzinsky, 1987). The chondrocytes maintain normal physiological mechanical behavior of cartilage by controlling the synthesis, assembly and turnover of the ECM, partly in response to mechanical factors (Helminen et al., 1987). It is the composition and structure of the ECM which in turn determines the biomechanical characteristics of the tissue. The molecular components of the ECM include collagens, proteoglycans, hyaluronan, and noncollagenous proteins and glycoproteins (Heinegard and Oldberg, 1989). The collagen network forms the extracellular skeleton around which other molecules are assembled. The predominant noncollagenous extracellular constituent is the proteoglycan, aggrecan. In general, the rope-like collagen fibrils endow cartilage with its mechanical strength in tension while the electrically charged gel-like aggrecan entrapped within the collagenous network provides resistance to compression (Buschmann and Grodzinsky, 1995). For example, the dramatic rise in compressive equilibrium stiffness of chondrocytes cultured in agarose occurred coincident with increased deposition of aggrecan in the gel (Buschmann et al., 1992).

The ability of mechanical stimuli to affect cartilage structure and metabolism is documented in animal studies, tissue explant systems, and cell culture models. Animal studies have shown that aggrecan concentration is often higher in areas of habitually loaded cartilage (Slowman and Brandt, 1986), and can be

further increased by increased dynamic physiological loading (Caterson and Lowther, 1978; Salter et al., 1980; Kiviranta et al., 1988). In contrast, immobilization of joints tends to decrease aggrecan concentration (Olah and Kostenszky, 1972; Akeson et al., 1973; Palmoski et al., 1979; Kiviranta et al., 1987). The observation that aggrecan content in the joint cartilage of animals can be reduced by excessive dynamic loading (Jurvelin et al., 1990) suggests that there are limits to the remodeling capacity of cartilage in its attempt to meet functional demands. The qualitative trends seen in these animal studies have been substantiated and amplified by in vitro explant models where a static equilibrium compression inhibits synthetic rates (Jones et al., 1982; Schneiderman et al., 1986; Gray et al., 1988; Sah et al., 1989) and dynamic nonequilibrium loading at certain amplitudes and frequencies can stimulate matrix production (Palmoski and Brandt, 1984; Copray et al., 1985; Sah et al., 1989; Larsson et al., 1991; Korver et al., 1992; Parkkinen et al., 1992; Kim et al., 1994). The phenotypically stable system of chondrocytes cultured in agarose has also exhibited inhibition of synthesis in response to static compression and stimulation of synthesis under dynamic compression (Buschmann et al., 1995a).

Many physical and chemical signals with potential effects on chondrocyte and ECM metabolism may be generated by tissue loading. Static equilibrium compression has been shown to: (1) reduce the rate of transport of macromolecules due to reduced average ECM pore size (Jones et al., 1982); (2) change ion concentrations including pH via the Donnan effect (Gray et al., 1988; Urban et al., 1993; Boustany et al., 1995) and (3) alter cell and nucleus structure (Freeman et al., 1994; Guilak et al., 1995; Guilak, 1995; Boustany et al., 1995; Buschmann et al., 1995b). Dynamic compression can additionally superimpose fluid flows, pressure gradients, and streaming currents or potentials (Mow et al., 1980; Frank and Grodzinsky, 1987; Kim et al., 1994, 1995). In vitro explant systems have the potential to be quantitative and specific in relating mechanical and biological parameters in addition to removing potential systemic effects or local inflammatory mediators present in animal studies. Our study focuses on potential relationships between cell and nucleus structure and aggrecan synthesis in statically compressed cartilage. We radiolabeled explanted and compressed cartilage disks with [^{35}S]sulfate, fixed them in the compressed state with glutaraldehyde and processed disks for quantitative autoradiography and light microscopy-based stereological estimations. We found, as have previous investigators, a reduction in total aggrecan synthesis with increasing static compression levels. However, we also found a compression-induced spatial gradient in aggrecan synthesis which was not present in free-swelling disks. Stereological measurements at the centre of disks showed a reduction in cell and nucleus volume, surface area, and radii in the direction of compression. These correlated changes in biosynthesis and stereological parameters suggest that alterations in cell and nuclear structure may be a primary mode by which chondrocytes detect and respond to changes in the mechanical environment.

MATERIALS AND METHODS

Isolation and culture of cartilage disks

Cylindrical cartilage disks, 3 mm in diameter and 1 mm thick, were explanted from the femoropatellar groove of 1- to 2-week-old calves and incubated in medium (DMEM with 10 mM Hepes, 10% (v/v) FBS, 0.1 mM nonessential amino acids, an additional 0.4 mM proline, and 20 μg/ml ascorbate) changed daily, as described previously (Sah et al., 1989). The thickness of these explanted cartilage disks increased to ~1.5 mm, but remained uniform with little curvature, after 1 day of free-swelling culture. This post-explant swelling was most likely due to cutting of the cartilage at all edges, and the swelling pressure associated with the high proteoglycan content of this young tissue. However, in contrast to adult articular cartilage, a significant advantage of this young tissue is that it is approximately homogeneous and isotropic in terms of cell and extracellular matrix structure, rendering detailed analysis more tractable in initial experiments.

Compression, radiolabeling, and fixation under compression

On days 3 and 5 post-explant, cartilage disks were subjected to graded levels of static, uniaxial, radially unconfined compression using previously described polysulphone chambers (Sah et al., 1989). Disks were compressed to the desired thickness between smooth impermeable platen surfaces of the base and lid of the compression chambers. In this unconfined geometry, the radial periphery of each disk could expand upon application of compression and then recoil and relax to reach the final equilibrium state (Jurvelin et al., unpublished). On each day of compression (day 3 and day 5 post-explant) 3 groups of 12 disks each were compressed to 1.0 mm, 0.75 mm, or 0.5 mm thickness, respectively, using one compression chamber for each thickness. A fourth group of 12 disks was placed in a compression chamber and held at the original ~1.5 mm thickness. After application of compression, culture medium supplemented with 10 μCi/ml [^{35}S]sulfate was added, and the compression chambers were transferred to an incubator for 12 hours. Previous equilibration in the incubator assured that the medium and chamber temperature were 37°C. After the 12 hour compression/radiolabeling period, the chambers were removed from the incubator and the radiolabeled medium was replaced with unlabelled medium, while maintaining the attained compression levels. Disks were washed three additional times with unlabelled medium over 1 hour total after which they were fixed in the compressed state by replacing the medium with 0.05 M sodium cacodylate buffer containing 2% (v/v) glutaraldehyde and 2.5% (w/v) cetylpyridinium chloride. After fixation at room temperature over 16 hours, the disks were removed from the compression chambers, washed with 0.1 M sodium cacodylate buffer 4 times over 2 hours, and then stored for up to 4 weeks in 70% ethanol at 4°C.

Quantitative autoradiography

Embedding, sectioning and quantitative autoradiography followed in detail the methods described previously (Buschmann et al., 1996). Since we wished to preserve spatial information regarding the depth and radius within cartilage disks from which autoradiographical and stereological measurements were made, we obtained vertical sections along the axis of disks. The fixed disks were therefore initially halved with a razor blade, dehydrated in a graded series of increasing ethanol concentrations, and embedded in Epon 812 which was polymerized at 60°C. Semi-thin 1 μm sections, obtained with an ultramicrotome, were taken from the cut face of one of the halves and were therefore rectangular in shape with a width equal to the disk diameter (~3 mm) and height equal to disk thickness (0.5-1.5 mm, depending on the compression level). Slides containing the sections were dipped in emulsion, exposed for 2 weeks, developed and fixed. Sections were lightly stained with 0.008% toluidine blue in buffer (2% boric acid, 1% sodium tetraborate, pH 7.6). Sections were viewed on a light microscope using a high power (100×) oil immersion objective and images were digitized and transferred to a personal computer via a CCD color camera. For each disk, a sequential series of 12-15 images in 100 μm increments was captured from the specimen center to the

radial periphery. The number of grains in each image was found by: (1) thresholding the image on the blue channel to isolate silver grains; (2) determining the average area of a single grain in the image using the lowest section of the histogram of grain size; and (3) dividing total grain area by the average size of a single grain. By comparison to scintillation counts, it was previously demonstrated that each disintegration occurring within the section during the exposure time resulted in 0.67±0.21 grains (mean ± standard deviation, n=58), independent of the density of grains (Buschmann et al., 1996). The average grain density for a particular image is therefore a direct measure of the amount of aggrecan synthesized during the 12 hour labeling period within the section volume associated with that image. The sequential series of digitized images allowed the characterization of aggrecan synthesis as a function of radial position within disks.

Stereological measurements of cell and nucleus structure

In contrast to the autoradiography measurements where we characterized aggrecan synthesis as a function of radial position within disks, stereological measurements were only made at disk centers, corresponding to radius = 0 in the autoradiography analysis. (Ongoing investigations are expanding the stereological characterization to include peripheral areas of disks.) The implemented stereological design accounted for the nonrandom, nonisotropic nature of vertical sectioning by using sine-weighted line probes for estimating volumes (Cruz Orive and Hunziker, 1986) or surface areas (Baddeley et al., 1986). All stereological measurements were made using black and white video printouts from a Mitsubishi video copy processor (model P78E) connected to the CCD camera on the microscope. Printouts (22.1 cm × 16.7 cm at a final magnification of 1870) were made from 4 adjacent regions in the center of each disk analyzed, representing a total rectangular area within the specimen of 0.24 mm wide × 0.18 mm high. Since specimen diameter was ~3 mm and specimen height was 0.5-1.5 mm, the stereology results pertain to a highly localized central area of the disks.

Absolute volume

Cell and nucleus volume were estimated using a modification of the nucleator (Gundersen, 1988; Gundersen et al., 1988; Moller et al., 1990). A guard frame of interior dimensions 14.1 cm × 12.7 cm was placed and centered on the video printout in order to exclude without bias cells for which intercepts could not be measured, i.e. cell profiles which extended beyond the area of the printout (Cruz Orive and Hunziker, 1986). We performed intercept measurements on cells and nuclei provided that the nuclear membrane was clearly visible on the section and that the center of the nucleus was within the guard frame. This sampling design strictly chooses cells and nuclei with a probability proportional to the height of the nucleus in the direction perpendicular to the section plane, the radial direction. Therefore calculated volumes (and radii) are rigorously defined as nuclear-height-weighted volumes (and radii). The difference between nuclear-height-weighted volumes and number-weighted volumes is in the order of a few percent (Moller et al., 1990). The reference point for classifying intercept lengths was chosen as the center of the nucleus profile, determined subjectively by the measurer. As pointed out previously, the nucleator estimate for particle volume is valid for any point within the object, so that our selection of the center of the nuclear profile as reference point does not introduce any bias (Gundersen, 1988; Gundersen et al., 1988).

Generation of isotropic line probes on vertical sections was accomplished by using an orientation grid with sine-weighting (Cruz Orive and Hunziker, 1986). The center of the orientation grid was located on the center of the nucleus, and a random number between the limits of the grid (1 to 97) was chosen to determine the direction of the line probe. The number 97 represented the horizontal direction towards the right and 0 the vertical direction. The lines were much more closely spaced near the horizontal direction compared to the vertical, in direct proportion to the sine of the angle with the vertical direction. (The need for this sine-weighting can be appreciated if one considers the use of non-sine-weighting. In three dimensions the latter would choose many more line probes, per unit solid angle, oriented near the vertical direction than near the horizontal direction due to the fact that the section always contains the vertical direction.) The distance between the nucleus center and the cell and nucleus membranes was measured by classifying the intercept lengths along the sine-weighted direction, for both + and − directions from the center, giving two intercepts for the cell (l_{cr+} and l_{cr-}) and two for the nucleus (l_{nr+} and l_{nr-}). The orientation grid was then flipped so that the direction 97 was horizontal to the left and cell (l_{cl+} and l_{cl-}), and nucleus intercepts (l_{nl+} and l_{nl-}), were classified again. Intercept length was recorded as (class number −0.5) representing the average length of intercepts in that class. After conversion of the intercept lengths to actual dimensions using a calibration ruler, an unbiased estimation of cell volume was calculated as:

$$v_C = \frac{\pi}{3}\,(l^3_{cr+} + l^3_{cr-} + l^3_{cr+} + l^3_{cr-})\,. \qquad (1)$$

For each of the four experimental groups (1.5 mm, 1 mm, 0.75 mm and 0.5 mm thickness), 6 disks were analyzed using 4 video printouts from the center of each disk. The total number of cells per disk for which v_C was obtained ranged from 8 to 23, and the final estimate of cell volume for a specimen was calculated as the mean. The mean and standard error for each experimental group was then calculated from the 6 estimated volumes. Nucleus volume was estimated following the same procedure as for cell volume.

Directional radius

Radii of the cell and the nucleus in the direction of compression (vertical radius) and perpendicular to the direction of compression (horizontal radius) were made from the same population of cells used to estimate cell and nucleus volume. The center of the nucleus profile was used again as the reference point for classifying intercepts in + and − directions. The only difference with respect to the volume intercepts was that radii were measured in predefined directions, namely horizontal (l_{ch+} and l_{ch-}) and vertical directions (l_{cv+} and l_{cv-}) for the cell and similarly for the nucleus. For each sampled cell the directional radii were calculated as the mean of the + and − radii. For example cell vertical radius was calculated as:

$$r_{CV} = \tfrac{1}{2}(l_{cv+} + l_{cv-})\,. \qquad (2)$$

The cell radii of each disk were calculated as the mean of the sampled cells (8-23) for each disk and the mean and standard error for each experimental group was found using the estimated radii from the 6 disks per group. As discussed above for volumes, the directional radii are more strictly defined as nuclear-height-weighted radii.

Volume fraction

Volume fractions were estimated using standard point-counting (Cruz Orive and Hunziker, 1986). A grid with regularly spaced points was placed on the video printout and the number of points falling within the reference volume (the entire printout), P_R, within cells, P_C, and within nuclei, P_N, were recorded. The same set of points was used for the cells and nuclei while a less dense set, by a factor of 16, was used for the reference volume. Three volume fractions were then calculated, the ratio of cell volume to tissue volume, f_C, the ratio of nucleus volume to tissue volume, f_N, and the ratio of nucleus volume to cell volume, f_{NC}, as:

$$f_C = \frac{P_C}{16P_R}\,; \qquad f_N = \frac{P_N}{16P_R}\,; \qquad f_{NC} = \frac{P_N}{P_C}\,. \qquad (3)$$

Density

The number density of cells and nuclei was estimated indirectly using

the measured volumes and volume fractions. Cell density, N_C, and nucleus density, N_N, were estimated as:

$$N_C = \frac{f_C}{v_C}\ ; \qquad N_N = \frac{f_N}{v_N}\ . \tag{4}$$

Surface area

The surface area per unit reference volume for cells and nuclei was estimated using cycloid arcs on vertical sections (Baddeley et al., 1986; Cruz Orive and Hunziker, 1986). A grid containing horizontally oriented cycloid arcs and a set of regularly spaced points was placed directly on the video printout (no guard frame). The number of intersections of the cycloid arcs and the cell membrane was recorded as I_C and the number of points falling in the reference frame (the entire video printout) was recorded as P_R. Using the calibration factor of the grid, λ = points per length of cycloid arc, the surface area of cell membrane per unit reference volume was calculated for each specimen using the sum of I_C and the sum of P_R for the 4 printouts per specimen, as:

$$S_{CV} = 2\lambda\ \frac{I_C}{P_R}\ . \tag{5}$$

The surface area per cell was then estimated as:

$$S_C = \frac{S_{CV}}{N_C}\ . \tag{6}$$

The surface area estimated here is defined as the light-microscope detectable surface area, since the resolution of the instrument (i.e. light vs electron microscope) can have an effect on the values obtained (higher resolution may result in higher measured surface area). The nuclear surface area was estimated in a similar manner.

RESULTS

Dimensional changes due to fixation, dehydration, embedding and sectioning

In order to characterize dimensional changes induced by fixation, dehydration, embedding, and sectioning, we measured the thickness of the cartilage disks at three different time points during processing (Table 1). The compressed thickness was determined by the thickness of Teflon spacers present in the compression chambers. After glutaraldehyde fixation in the compressed state, release from compression and placement in 70% ethanol, thickness of disks was measured with a micrometer. After dehydration, embedding and sectioning, we again measured the section thickness using digitized light microscope images. The results indicated that the compressed state was adequately maintained (±2% in thickness) by the glutaraldehyde fixation, with one exception: the disks subjected to the highest level of compression (1.5 mm → 0.5 mm) reswelled following release from compression by ~30% in thickness. Dimensional changes induced by dehydration, embedding, and sectioning were small but slightly larger than those induced by release from compression (±10% in thickness). Only the 10% shrinkage of the free-swelling specimen was statistically significant (P<0.05; two-tailed t-test). The ~10% linear shrinkage seen in the uncompressed (1.5 mm thickness) and 1.0 mm compressed thickness disks is similar to that observed previously (Hunziker and Schenk, 1989). Taken together, these results indicate that the magnitude of dimensional changes induced by the various processing stages is small compared to magnitude of the imposed reduction in tissue thickness.

Table 1. Tissue dimensional changes during processing

Processing stage				
Compressed thickness (mm)	1.5	1.0	0.75	0.5
Post-fixation and post-release thickness (mm)	1.48±0.07	0.98±0.07	0.76±0.02	0.65±0.04
% Change in thickness due to release from compression after fixation	−1	−2	+1	+30
Post-embedding and post-sectioning thickness (mm)	1.33±0.12	0.86±0.09	0.80±0.05	0.65±0.08
% Change in thickness due to embedding and sectioning	−10	−12	+5	0
Total % change in thickness	−11	−14	+7	+30

Compressed thickness was determined by the thickness of Teflon spacers in specially designed compression chambers (Sah et al., 1989). After glutaraldehyde fixation in the presence of cetylpyridinium chloride followed by release of the specimens from the compression chambers and placement in 70% ethanol, the thickness of the specimens was measured with a micrometer. The thickness was measured again following embedding and sectioning by imaging the section at low power on the light microscope. The results indicated that dimensional changes during preparative procedures were generally minimal. Exceptions to this trend were seen in the highly compressed specimen (0.5 mm thickness) where release from the chamber after fixation resulted in swelling of 30%. Mean ± s.d. (n=6).

Reduction of aggrecan synthesis due to compression exhibits a spatial dependence

A previously developed quantitative autoradiographic method (Buschmann et al., 1996) was used to estimate the rate of aggrecan synthesis within cartilage disks during compression and as a function of radial position within the disk. Axial variation of aggrecan synthesis appeared qualitatively to be less significant than radial variation and was not characterized. Exemplar micrographs of developed autoradiographic sections are shown in Fig. 1, demonstrating qualitatively both the reduced synthesis due to increasing compression levels and the spatial gradient in synthesis for compressed specimens. The grain density is lower in the center than at the edge for compressed specimens (Fig. 1C vs D, E vs F, G vs H). The qualitative impression of the micrographs in Fig. 1 was born out quantitatively by the results of the grain counting procedure shown in Fig. 2. The free-swelling specimens displayed an approximately uniform grain density. Increasing compression reduced aggrecan synthesis at each radial position and introduced a radial gradient in synthesis within the disks. For example, the disks compressed axially by 33% demonstrated ~30% reduction in synthesis on average within disks but this reduction varied from ~50% at the center to ~15% near the periphery (Fig. 2). With increasing compression levels, synthesis was further reduced while maintaining the radial gradient in synthesis.

Cell and nucleus volume, surface area, and vertical radius are reduced by compression

Representative micrographs taken from the centers of compressed tissue specimens, similar to those from which stereological measurements were made, are shown in Fig. 3. Quali-

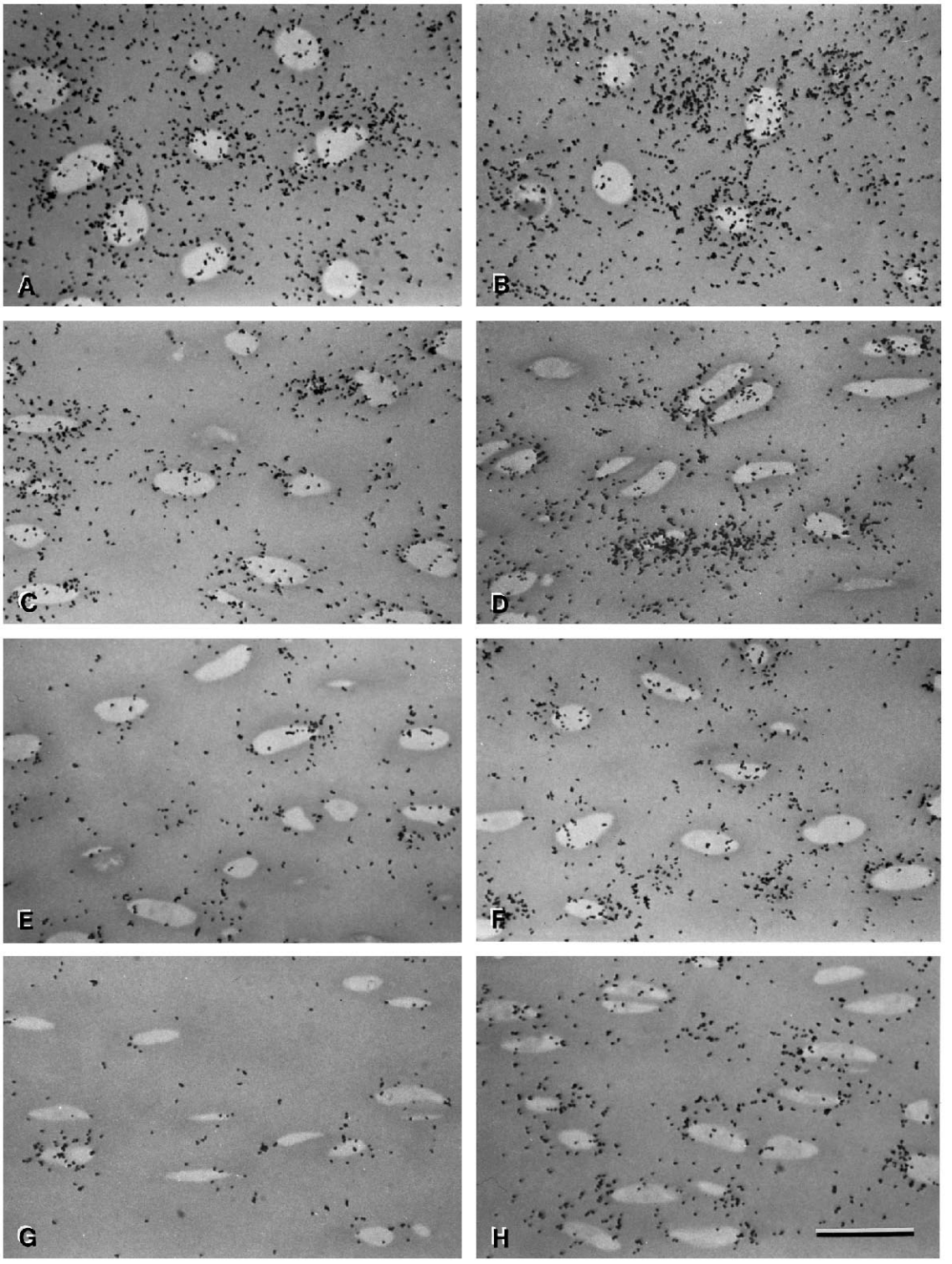

Fig. 1. Light micrographs of autoradiography sections. Cartilage disks were labeled during the 12 hour compression and fixed with glutaraldehyde in the compressed state. [^{35}S]sulfate incorporation into aggrecan results in silver grains on these lightly stained (0.008% toluidine blue) 1 μm thick Epon sections. (A and B) Free-swelling, ~1.5 mm thick; (C and D) 1.0 mm compressed thickness; (E and F) 0.75 mm compressed thickness; (G and H) 0.5 mm compressed thickness. A, C, E and G are taken at the specimen centers, while B, D, F, and H are taken near the disk periphery. Digitized images from these regions and intermediate regions were used to count grains and quantitate the amount of aggrecan synthesized as a function of position within the disks (Fig. 2). Bar, 20 μm.

tative impressions from these micrographs suggested that increasing compression altered cell and nucleus shape and may have reduced their volumes. In addition, staining of the nucleus with toluidine blue was also consistently darker with increasing compression. Quantitative stereological characterization showed that cell and nucleus volume and surface area were indeed reduced by static compression (Fig. 4). Volumes of cells and nuclei were reduced approximately in proportion to the reduction in disk thickness imposed by the compression (Fig. 4A). Reductions in the surface area of cells and nuclei were slightly less than proportional to reduced thickness (Fig. 4B).

Cell and nucleus radii in the direction of compression (vertical) were reduced by compression, while cell and nucleus radii perpendicular to the direction of compression (horizontal) appeared to be largely unaffected (Fig. 5). The reductions

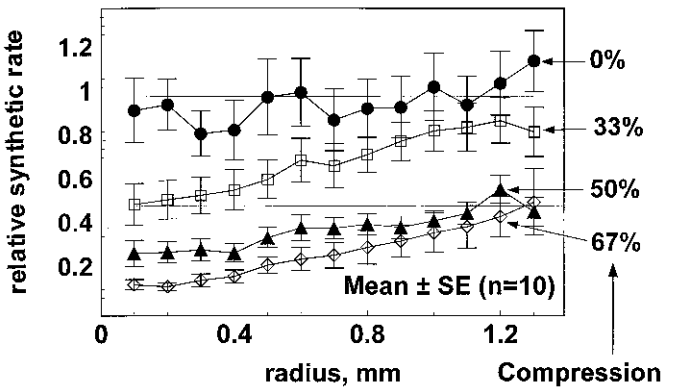

Fig. 2. Relative synthetic rates of aggrecan in compressed cartilage disks as a function of radial position (0 mm, disk center; 1.4 mm, disk periphery). A grain counting procedure was applied to digitized images, similar to those of Fig. 1, to estimate aggrecan synthetic rate as a function of radial position in compressed cartilage disks. The grain densities were normalized to the average grain density in the uncompressed free-swelling specimens. Aggrecan synthesis in uncompressed specimens of this young calf tissue is approximately spatially uniform. Increasing levels of static compression reduce the rate of aggrecan synthesis. The reduction is stronger in the center of disks compared to the periphery.

in cell and nucleus radii in the vertical direction were approximately in proportion to the reduction in disk thickness imposed by the compression. While the volume fractions of cells and nuclei exhibited a slight decrease due to compression (Fig. 6A), this decrease was only statistically significant ($P<0.05$; two-tailed *t*-test) when comparing the highest compression level (0.5 mm thickness) to free-swelling (1.5 mm thickness), resulting in a 27% decrease in cell volume fraction. The nucleus to cell volume fraction did not change significantly (Fig. 6B).

Cell and nucleus number density increased in approximate inverse proportion to the reduction in disk thickness imposed by compression (Fig. 7). The slight difference in cell and nucleus number density reflects the indirect nature of this estimator since it was calculated by combining information obtained from point counting and from intercept measurements. Different cell populations are used when point-counting versus measuring intercept lengths resulting in higher variation in the ratio estimator of Equation 4.

DISCUSSION

As part of long term objectives investigating mechanical transduction in health and disease in cartilage, the goal of our present study was to characterize changes in aggrecan synthesis and in cell and nucleus structure in articular cartilage subjected to static compression. Aggrecan is a well-characterized ECM constituent whose primary functional role is well-established: it endows cartilage with its high resis-

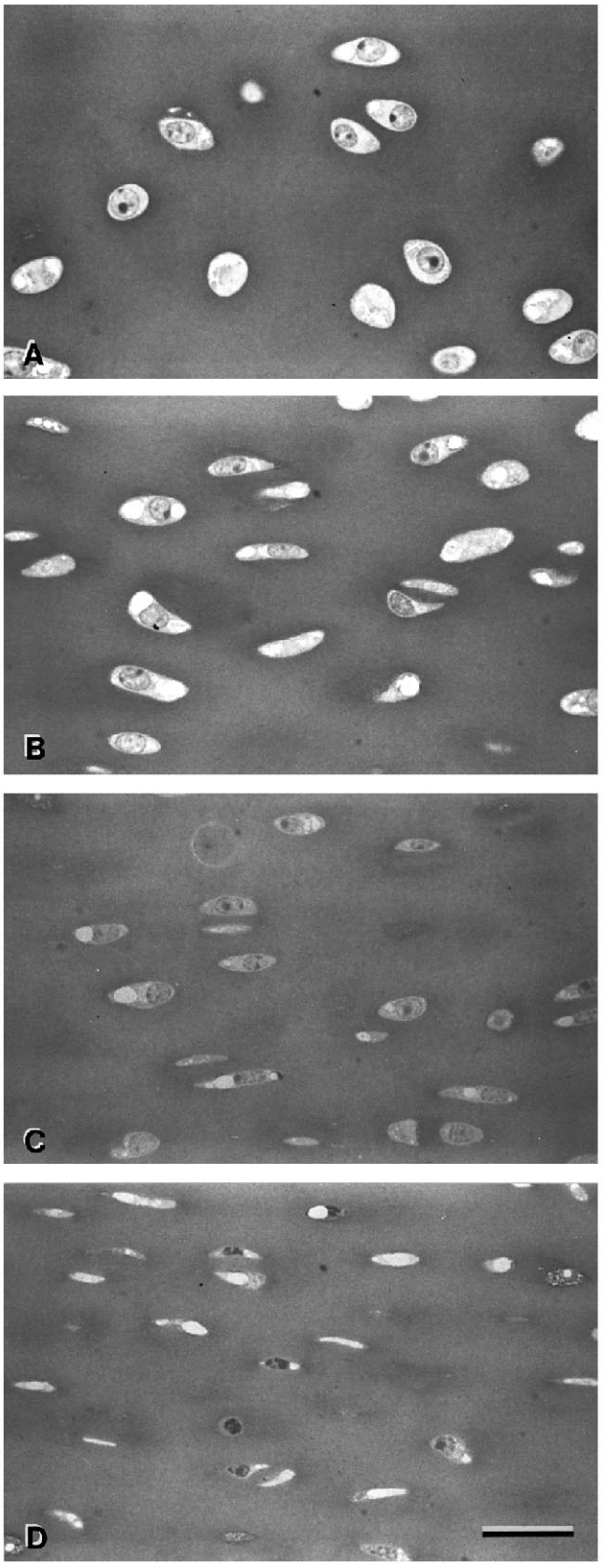

Fig. 3. Light micrographs taken from similar regions as the video printouts used for stereological evaluation. Sections from the same embedded specimens as those used for autoradiography (Fig. 1) were stained with 1% toluidine blue. (A) Free-swelling, ~1.5 mm thick; (B) 1.0 mm compressed thickness; (C) 0.75 mm compressed thickness; (D) 0.5 mm compressed thickness. Cell and nucleus deformation is evident. The presence of darkly stained nuclei and an increased incidence of vacuoles was consistently observed for the highly compressed specimens (D, 0.5 mm compressed thickness). Bar, 20 μm.

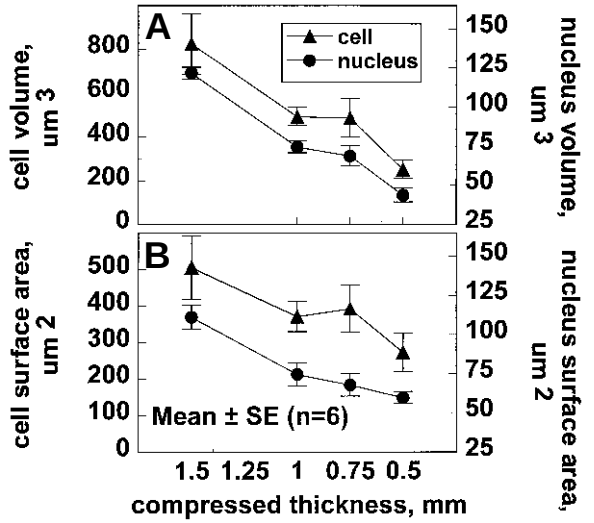

Fig. 4. Cell and nucleus volume (A) and cell and nucleus surface area (B) as a function of compressed thickness. These structural parameters were measured using stereological methods. The volume and surface area of cells and of nuclei are decreased with increasing compression. The reduction in volume of cells and nuclei is approximately in proportion to the reduction in disk thickness by the imposed compression. The percentage reduction of surface area of cells and nuclei is generally less than the percentage reduction of disk thickness.

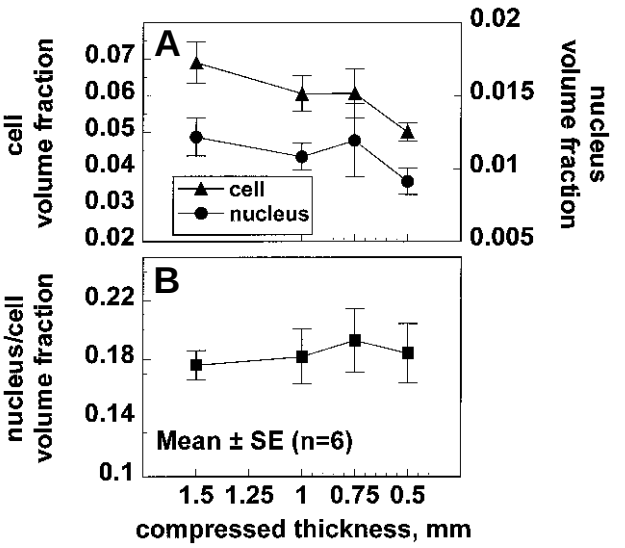

Fig. 6. Cell and nucleus volume fractions (relative to tissue volume) (A) and nucleus to cell volume fraction (nucleus volume divided by cell volume) (B) as a function of compressed thickness. These structural parameters were measured using stereological methods. An apparent slight decrease in cell and nucleus volume fractions was observed due to compression, although only the 27% decrease in cell volume fraction from free-swelling, ~1.5 mm thickness, to 0.5 mm compressed thickness was statistically significant ($P<0.05$; two-tailed *t*-test).

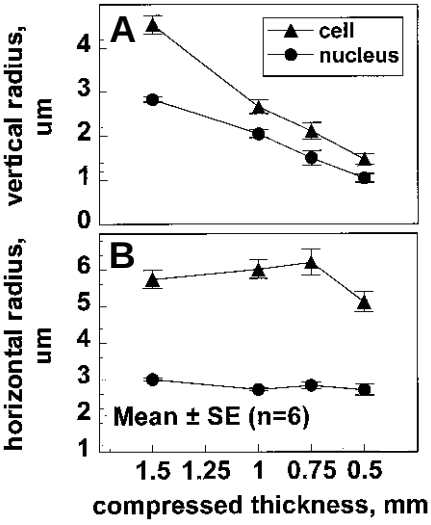

Fig. 5. Cell and nucleus vertical radius (A) and cell and nucleus horizontal radius (B) as a function of compressed thickness. These structural parameters were measured using stereological methods. The vertical radius (in the direction of compression) of cells and of nuclei is decreased with increasing compression. The horizontal radius (in the direction perpendicular to compression) of cells and nuclei is not significantly affected by compression. The reduction in vertical radius of cells and nuclei is approximately in proportion to the reduction in disk thickness by the imposed compression.

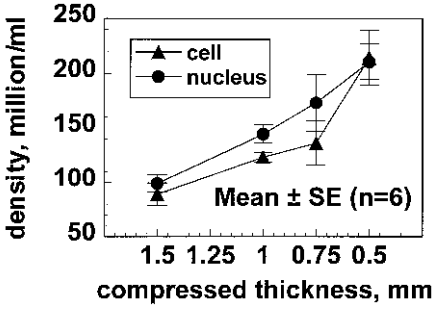

Fig. 7. Cell and nucleus number density as a function of compressed thickness. These structural parameters were measured using stereological methods. Both cell and nucleus number density increase in approximately inverse proportion to compressed thickness. The slight difference in cell and nucleus densities reflects the indirect method of measurement combining intercept measurements with volume fractions (Equation 4).

tance to compressive forces. Therefore changes in aggrecan synthesis may represent physiological adaptation to an altered mechanical environment. Moreover, a recently established quantitative autoradiography procedure allowed the characterization of aggrecan synthesis as a function of position within tissue pieces. Applying this autoradiography technique and stereological methodology to compressed, radiolabelled and chemically fixed disks, we found that static compression reduces aggrecan synthesis as well as cell and nucleus volume, surface area, and radius in the direction of compression. These results constitute the first demonstration of a correlation between altered cell and nucleus structure and a physiological response representing functional adaptation in loaded cartilage.

Static compression induces a radial gradient superimposed on a net reduction of aggrecan synthesis in unconfined geometry

The quantitative autoradiography data (Figs 1 and 2) showed that aggrecan synthesis decreased monotonically with increasing static compression at each radial position within the disks. In addition, aggrecan synthesis exhibited a significant gradient in the radial direction at each applied compression level (Fig. 2). This data is consistent with the results of separate experiments from a recent study (Kim et al., 1994), where we found a radial gradient of aggrecan synthesis in statically compressed cartilage disks, by coring 2 mm disks out of 3 mm disks and using scintillation counting on the central disks and outer rings. Although quantitative grain counting in the axial direction was not performed, qualitative examination indicated little inhomogeneity in aggrecan synthesis in the axial direction. The uncompressed disks, which were not covered by impermeable platens on their upper surface displayed a relatively uniform rate of aggrecan synthesis throughout the specimen, independent of radial (Fig. 2) or axial position. The compression-induced radial gradient of aggrecan synthesis (more inhibition in the center than near the edge) may be related to several phenomena including: (1) compression-induced transport limitations; (2) radial inhomogeneity in tissue strain or stress at equilibrium; or (3) a biosynthetic response to the initial mechanical transient involving fluid flow and radial inhomogeneity in tissue strain and stress prior to equilibrium.

Transport limitations may be induced due to the reduction in tissue pore size under compression. Such tissue compaction could potentially affect diffusion to and from the specimen's interior of small molecules such as SO_4^{2-} and amino acids, as well as endogenous macromolecules or macromolecules present in serum-supplemented medium. Diffusion limitations might thereby contribute to the decrease in sulfate incorporation at the center compared to the radial periphery, at each compression level (Fig. 2). However, since sulfate incorporation decreased with compression at all radial positions, including the periphery, it is unlikely that transport limitations are the main cause of reduced biosynthesis by compression. This conclusion is supported by extensive control studies reported recently (Kim et al., 1994). In addition, inhibition of proteoglycan synthesis by static compression has been observed in explants of widely varying dimensions, from 200 μm slices (Schneiderman et al., 1986) to the 3 mm diameter disks used in our studies. If diffusion limitations were important, one might expect to see systematic differences between experiments utilizing tissues of such different dimensions, since diffusion times are proportional to the square of the path length over which transport occurs. In recent studies involving chondrocytes cultured in 3 mm diameter agarose disks (Buschmann et al., 1995a) we observed spatially uniform aggrecan synthesis under free swelling conditions, while static compression again induced radial gradients in synthesis. In the agarose system, chondrocytes were present at a cell density of ~20% that of the explant. Potential intratissue gradients in oxygen or lactate should therefore be quite different in the agarose and explant systems. However, the two systems respond to compression in a very similar manner. Nevertheless, other tissue systems having larger dimensions may exhibit important intratissue gradients in lactate or oxygen (Stairmand et al., 1991; Ohshima and Urban, 1992).

The second hypothesized cause of the radial gradient in aggrecan synthesis is related to differences in equilibrium tissue strains or stresses at the tissue center versus those at the periphery. Ongoing measurements of cell and nucleus structure as a function of radial position may indicate whether ECM strain changes as a function of radial position. Preliminary data suggest that a radial inhomogeneity in cell and nucleus structure may exist, but appears to be small. Mechanical models of deformations in the small strain limit within an isotropic poroelastic material indicate that tissue strain and stress should be uniform at equilibrium (Kim et al., 1995). Some assumptions inherent in this model may, however, not be satisfied by our relatively large static strain amplitude experiments. Although geometric nonlinearities implicated by the finite strain applied should not induce gradients in tissue stress or strain, material nonlinearities could have surprising effects. In this context the third hypothesized phenomenon involving the initial transient phase of tissue compression may be important. The large amplitude of strain imposed will initially induce relatively large interstitial fluid flows, pressures and solid matrix stress and strain. This initial transient could either be the cause of inhomogeneities in tissue stress and strain at equilibrium, or even in their absence, a longer term cell response due to the transient period could be induced. Although definitive data are not yet available, the above considerations suggest that a mechanical source of the compression-induced gradient in aggrecan synthesis may be more likely than mechanisms related to transport limitations.

Cell and nucleus deformation at equilibrium follows imposed tissue deformation

Uniaxial compression of calf cartilage disks in unconfined geometry probably induces an initial radial expansion followed by a recoil and relaxation of the unconstrained periphery of the disks, as has been observed in more mature cartilage (Jurvelin et al., unpublished). By measuring projected areas (data not shown) of compressed and chemically fixed disks with the microscope we found that disk recoil in the radial direction was nearly complete so that disk diameter, at equilibrium, changed very little with the increasing levels of compression used in this study (the equilibrium Poisson's ratio calculated from these measurements of projected disk areas under graded levels of compression was in the range 0.01-0.1). In the radial direction we also observed minimal changes in cell and nucleus horizontal radii (Fig. 5B). In contrast, vertical radii of cells and nuclei decreased in approximately the same proportion as imposed reductions in disk thickness (Fig. 5A). Our studies therefore lend support to a general rule that cell and nucleus shape in loaded cartilage follow shape changes imposed on external tissue surfaces, at least at equilibrium after the cessation of fluid exudation from the tissue. Previous studies characterizing cell or nucleus deformation in compressed cartilage are consistent with this finding (Boustany et al., 1995; Guilak, 1995).

Rate of aggrecan synthesis correlates with cell and nucleus volumes, surface areas, and vertical radii in statically compressed cartilage: Possible molecular mechanisms

Comparison of changes in aggrecan synthesis at the center of cartilage disks to changes in cell and nucleus structure at the

same location showed that aggrecan synthesis was reduced simultaneously with reductions in cell and nucleus volumes, and surface areas, and vertical radii. Based on these data alone, however, it is difficult to establish a direct cause and effect relationship between biosynthesis and any one structural parameter. Ongoing studies are directed at this issue. Nevertheless, the distinct correlation between changes in aggrecan synthesis and general cell and nucleus structure presented here serves to highlight a number of potentially important control points and molecular mechanisms which may link synthesis to structure of the cell or nucleus.

The chondrocyte/extracellular-matrix interface bears integrin (Durr et al., 1993; Enomoto et al., 1993) and hyaluronan receptors (Knudson and Knudson, 1993). The cytoplasmic domain of integrin receptors is linked directly to the cell cytoskeleton and possesses a tyrosine kinase activity (Burridge et al., 1992). Mechanical perturbations at the cell membrane may therefore be transduced mechanically or chemically to alter biosynthesis at various levels potentially involving phosphorylation cascades (Hershey, 1991), mRNA-cytoskeletal interactions (Singer, 1992; Hesketh and Pryme, 1991), and microtubule mediated export (Vale, 1987). In addition to the cytoplasmically located mechanisms, our data show that tissue and cell deformation can be directly translated to nuclear deformation. Although we do not know whether this nuclear deformation involves biochemical mediation by the cell, it is possible that it is primarily controlled by the mechanics of the cytoskeleton (Sims et al., 1992) and nucleoskeleton (Spector, 1993). Intermediate filaments may be important in this regard given their network formation spanning between and potentially linking nucleus and cell membranes (Goldman et al., 1985; Georgatos and Blobel, 1987). Nuclear size has also been shown to increase in response to growth factor stimulation (Yen and Pardee, 1979; Ingber et al., 1987) and one potential regulatory point may be nucleocytoplasmic transport regulated by nuclear pore complexes (Jiang and Schindler, 1988; Pante and Aebi, 1993). Direct alteration of chromatin conformation is another potential regulatory control point. The noncondensed, open, nature of active chromatin may be caused by a number of factors such as locus control regions (Dillon and Grosveld, 1993) and nuclear matrix attachment sites (Cook, 1989). Potential mechanical regulation of biosynthesis at the transcriptional level through deformation of chromatin structure is implicated by our reduced nucleus volume under compression and the increased toluidine blue stain intensity seen in the nuclei of chondrocytes in compressed tissue. Such mechanical regulation of transcription via alterations in chromatin structure has been suggested previously. It was proposed that histone acetylation poises genes for activation and that mechanical torsion in the supercoiled DNA double helix, induced by nuclear topoisomerases, triggers gene activation (Ausio, 1992). An analogous mechanism may be at work in the chondrocyte response to mechanical loading. The triggering function of topoisomerase-induced torsion may be replaced by direct mechanical deformation of the cell and nucleus. In the case of static compression, net volume reduction of the nucleus may lead to a more condensed chromatin state and inhibition of biosynthesis, while dynamic oscillatory compression which can stimulate biosynthesis may induce local cell and nucleus expansion (Buschmann et al., 1995c).

This research was supported by the AO/ASIF Foundation (93-G46), Switzerland, NIH Grant AR33236 and The Medical Research Council of Canada.

REFERENCES

Akeson, W. H., Woo, S. L., Amiel, D., Coutts, R. D. and Daniel, D. (1973). The connective tissue response to immobility: biochemical changes in periarticular connective tissue of the immobilized rabbit knee. *Clin. Orthop.* **93**, 356-362.

Ausio, J. (1992). Structure and dynamics of transcriptionally active chromatin. *J. Cell Sci.* **102**, 1-5.

Baddeley, A. J., Gundersen, H. J. G. and Cruz Orive, L. M. (1986). Estimation of surface area from vertical sections. *J. Microsc*. **142**, 259-276.

Boustany, N. N., Gray, M. L., Black, A. C. and Hunziker, E. B. (1995). Correlation between the synthetic activity and glycosaminoglycan concentration in epiphysial cartilage raises questions about the regulatory role of interstitial pH. *J. Orthop. Res.* **13**, 733-739.

Burridge, K., Turner, C. E. and Romer, L. H. (1992). Tyrosine phosphorylation of paxillin and pp125^{FAK} accompanies cell adhesion to extracellular matrix: A role in cytoskeletal assembly. *J. Cell Biol*. **119**, 893-903.

Buschmann, M. D., Gluzband, Y. A., Grodzinsky, A. J., Kimura, J. H. and Hunziker, E. B. (1992). Chondrocytes in agarose culture synthesize a mechanically functional extracellular matrix. *J. Orthop. Res.* **10,** 745-758.

Buschmann, M. D., Gluzband, Y. A., Grodzinsky, A. J. and Hunziker, E. B. (1995a). Mechanical compression modulates matrix biosynthesis in chondrocyte/agarose culture. *J. Cell Sci.* **108**, 1497-1508.

Buschmann, M. D. and Grodzinsky, A. J. (1995). A molecular model of proteoglycan-associated electrostatic forces in cartilage mechanics. *J. Biomech. Eng*. **117**, 179-192.

Buschmann, M. D., Hunziker, E. B., Kim Y. J. and Grodzinsky, A. J. (1995b). Coordinated changes in biosynthesis and morphology of cells and nuclei in articular cartilage under compression. *Trans. Orthop. Res. Soc.* **20**, 289.

Buschmann, M. D., Kim Y. J., Hunziker, E. B. and Grodzinsky, A. J. (1995c). Stimulated aggrecan synthesis correlates with expansive solid matrix strain and increased fluid flow in dynamically compressed cartilage. *Trans. Combined Orthop. Res. Soc.* **2**, 117.

Buschmann, M. D., Maurer, A. M., Berger, E. and Hunziker, E. B. (1996). A method of quantitative autoradiography for the spatial localization of proteoglycan synthesis rates in cartilage. *J. Histochem. Cytochem.* (in press).

Caterson, B. and Lowther, D. A. (1978). Changes in the metabolism of the proteoglycans from sheep articular cartilage in response to mechanical stress. *Biochim. Biophys. Acta* **540**, 412-422.

Cook, P. R. (1989). The nucleoskeleton and the topology of transcription. *Eur. J. Biochem*. **185**, 487-501.

Copray, J. C., Jansen, H. W. and Duterloo, H. S. (1985). Effects of compressive forces on proliferation and matrix synthesis in mandibular condylar cartilage of the rat in vitro. *Arch. Oral Biol*. **30**, 299-304.

Cruz Orive, L. M. and Hunziker, E. B. (1986). Stereology for anisotropic cells: Application to growth cartilage. *J. Microsc*. **143**, 47-80.

Dillon, N. and Grosveld, F. (1993). Transcriptional regulation of multigene loci: Multilevel control. *Trends Genet.* **9**, 134-137.

Durr, J., Goodman, S., Potocnik, A., Vondermark, H. and Vondermark, K. (1993). Localization of β-1-integrins in human cartilage and their role in chondrocyte adhesion to collagen and fibronectin. *Exp. Cell Res.* **207**, 235-244.

Enomoto, M., Leboy, P. S., Menko, A. S. and Boettiger, D. (1993). β-1 Integrins mediate chondrocyte interaction with type-I collagen, type-II collagen, and fibronectin. *Exp. Cell Res*. **205**, 276-285.

Frank, E. H. and Grodzinsky, A. J. (1987). Cartilage electromechanics I. Electrokinetic transduction and the effects of electrolyte pH and ionic strength. *J. Biomech.* **20**, 615-627.

Freeman, P. M., Natarajan, R. N., Kimura, J. H. and Andriacchi, T. P. (1994). Chondrocyte cells respond mechanically to compressive loads. *J. Orthop. Res.* **12**, 311-20.

Georgatos, S. D. and Blobel, G. (1987). Two distinct attachment sites for vimentin along the plasma membrane and the nuclear envelope in avian erythrocytes: A basis for a vectorial assembly of intermediate filaments. *J. Cell Biol.* **105**, 105-115.

Goldman, R., Goldman, A., Green, K., Jones, J., Lieska, N. and Yang, H. Y. (1985). Intermediate filaments: Possible functions as cytoskeletal connecting links between the nucleus and the cell surface. *Ann. NY Acad. Sci.* **455**, 1-17.

Gray, M. L., Pizzanelli, A. M., Grodzinsky, A. J. and Lee, R. C. (1988). Mechanical and physiochemical determinants of the chondrocyte biosynthetic response. *J. Orthop. Res.* **6**, 777-792.

Guilak, F. (1995). Transmission of extracellular matrix deformation to the chondrocyte nucleus via the actin cytoskeleton. *Trans. Orthop. Res. Soc.* **20**, 89.

Guilak, F., Ratcliffe, A. and Mow, V. C. (1995). Chondrocyte deformation and local tissue strain in articular cartilage: A confocal microscopy study. *J. Orthop. Res.* **13**, 410-421.

Gundersen, H. J. (1988). The nucleator. *J. Microsc.* **151**, 3-21.

Gundersen, H. J., Bagger, P., Bendtsen, T. F., Evans, S. M., Korbo, L., Marcussen, N., Moller, A., Nielsen, K., Nyengaard, J. R., Pakkenberg, B. and et al. (1988). The new stereological tools: disector, fractionator, nucleator and point sampled intercepts and their use in pathological research and diagnosis. *APMIS* **96**, 857-881.

Heinegard, D. and Oldberg, A. (1989). Structure and biology of cartilage and bone matrix noncollagenous macromolecules. *FASEB J.* **3**, 2042-2051.

Helminen, H. J., Kiviranta, I., Tammi, M., Saamanen, A., Paukkonen, K. and Jurvelin, J. (1987). *Joint Loading: Biology and Health of Articular Structures*. Bristol: Wright.

Hershey, J. W. (1991). Translational control in mammalian cells. *Annu. Rev. Biochem.* **60**, 717-755.

Hesketh, J. E. and Pryme, I. F. (1991). Interaction between mRNA, ribosomes and the cytoskeleton. *Biochem. J.* **277**, 1-10.

Hunziker, E. B. and Schenk, R. K. (1989). Physiological mechanisms adopted by chondrocytes in regulating longitudinal bone growth in rats. *J. Physiol.* **414**, 55-71.

Ingber, D. E., Madri, J. A. and Folkman, J. (1987). Endothelial growth factors and extracellular matrix regulate DNA synthesis through modulation of cell and nuclear expansion. *In Vitro Cell Dev. Biol.* **23**, 387-394.

Jiang, L. W. and Schindler, M. (1988). Nuclear transport in 3T3 fibroblasts: Effects of growth factors, transformation and cell shape. *J. Cell Biol.* **106**, 13-19.

Jones, I. L., Klamfeldt, A. and Sandstrom, T. (1982). The effect of continuous mechanical pressure upon the turnover of articular cartilage proteoglycans in vitro. *Clin. Orthop.* **165**, 283-289.

Jurvelin, J., Kiviranta, I., Saamanen, A. M., Tammi, M. and Helminen, H. J. (1990). Indentation stiffness of young canine knee articular cartilage--influence of strenuous joint loading. *J. Biomech.* **23**, 1239-1246.

Kim, Y. J., Sah, R. L. Y., Grodzinsky, A. J., Plaas, A. H. K. and Sandy, J. D. (1994). Mechanical regulation of cartilage biosynthetic behavior: physical stimuli. *Arch. Biochem. Biophys.* **311**, 1-12.

Kim, Y. J., Bonasser, L. J. and Grodzinsky, A. J. (1995). The role of cartilage streaming potential, fluid flow and pressure in the stimulation of chondrocyte biosynthesis during dynamic compression. *J. Biomech.* **28**, 1055-1066.

Kiviranta, I., Jurvelin, J., Tammi, M., Saamanen, A. M. and Helminen, H. J. (1987). Weight bearing controls glycosaminoglycan concentration and articular cartilage thickness in the knee joints of young beagle dogs. *Arthritis Rheum.* **30**, 801-809.

Kiviranta, I., Tammi, M., Jurvelin, J., Saamanen, A. M. and Helminen, H. J. (1988). Moderate running exercise augments glycosaminoglycans and thickness of articular cartilage in the knee joint of young beagle dogs. *J. Orthop. Res.* **6**, 188-195.

Knudson, C. B. and Knudson, W. (1993). Hyaluronan-binding proteins in development, tissue homeostasis and disease. *FASEB J.* **7**, 1233-1241.

Korver, T. H., van de Stadt, R. J., Kiljan, E., van Kampen, G. P. and van der Korst, J. K. (1992). Effects of loading on the synthesis of proteoglycans in different layers of anatomically intact articular cartilage in vitro. *J. Rheumatol.* **19**, 905-912.

Larsson, T., Aspden, R. M. and Heinegard, D. (1991). Effects of mechanical load on cartilage matrix biosynthesis in vitro. *Matrix* **11**, 388-394.

Moller, A., Strange, P. and Gundersen, H. J. (1990). Efficient estimation of cell volume and number using the nucleator and the disector. *J. Microsc.* **159**, 61-71.

Mow, V. C., Kuei, S. C., Lai, W. M. and Armstrong, C. G. (1980). Biphasic creep and stress relaxation of articular cartilage in compression: Theory and experiments. *J. Biomech. Eng.* **102**, 73-84.

Mow, V. C., Holmes, M. H. and Lai, W. M. (1984). Fluid transport and mechanical properties of articular cartilage: A review. *J. Biomech.* **17**, 377-394.

Ohshima, H. and Urban, J. P. (1992). The effect of lactate and pH on proteoglycan and protein synthesis rates in the intervertebral disc. *Spine* **17**, 1079-1082.

Olah, E. H. and Kostenszky, K. S. (1972). Effect of altered functional demand on the glycosaminoglycan content of the articular cartilage of dogs. *Acta Biol. Acad. Sci. Hung.* **23**, 195-200.

Palmoski, M., Perricone, E. and Brandt, K. D. (1979). Development and reversal of a proteoglycan aggregation defect in normal canine knee cartilage after immobilization. *Arthritis Rheum.* **22**, 508-517.

Palmoski, M. J. and Brandt, K. D. (1984). Effects of static and cyclic compressive loading on articular cartilage plugs in vitro. *Arthritis Rheum.* **27**, 675-681.

Pante, N. and Aebi, U. (1993). The nuclear pore complex. *J. Cell Biol.* **122**, 977-984.

Parkkinen, J. J., Lammi, M. J., Helminen, H. J. and Tammi, M. (1992). Local stimulation of proteoglycan synthesis in articular cartilage explants by dynamic compression in vitro. *J. Orthop. Res.* **10**, 610-620.

Sah, R. L., Kim, Y. J., Doong, J. Y., Grodzinsky, A. J., Plaas, A. H. and Sandy, J. D. (1989). Biosynthetic response of cartilage explants to dynamic compression. *J. Orthop. Res.* **7**, 619-636.

Salter, R. B., Simmonds, D. F., Malcolm, B. W., Rumble, E. J., MacMichael, D. and Clements, N. D. (1980). The biological effect of continuous passive motion on the healing of full-thickness defects in articular cartilage. *J. Bone Joint Surg.* **62**, 1232-1251.

Schneiderman, R., Keret, D. and Maroudas, A. (1986). Effects of mechanical and osmotic pressure on the rate of glycosaminoglycan synthesis in the human adult femoral head cartilage: An in vitro study. *J. Orthop. Res.* **4**, 393-408.

Sims, J. R., Karp, S. and Ingber, D. E. (1992). Altering the cellular mechanical force balance results in integrated changes in cell, cytoskeletal and nuclear shape. *J. Cell Sci.* **103**, 1215-1222.

Singer, R. H. (1992). The cytoskeleton and mRNA localization. *Curr. Opin. Cell Biol.* **4**, 15-19.

Slowman, S. D. and Brandt, K. D. (1986). Composition and glycosaminoglycan metabolism of articular cartilage from habitually loaded and habitually unloaded sites. *Arthritis Rheum.* **29**, 88-94.

Spector, D. L. (1993). Macromolecular domains within the cell nucleus. *Annu. Rev. Cell Biol.* **9**, 265-315.

Stairmand, J. W., Holm, S. and Urban, J. P. (1991). Factors influencing oxygen concentration gradients in the intervertebral disc. A theoretical analysis. *Spine* **16**, 444-449.

Urban, J. P., Hall, A. C. and Gehl, K. A. (1993). Regulation of matrix synthesis rates by the ionic and osmotic environment of articular chondrocytes. *J. Cell. Physiol.* **154**, 262-270.

Vale, R. D. (1987). Intracellular transport using microtubule-based motors. *Annu. Rev. Cell Biol.* **3**, 347-378.

Yen, A. and Pardee, A. B. (1979). Role of nuclear size in cell growth initiation. *Science* **204**, 1315-1317.

(Received 25 August 1995 - Accepted 15 November 1995)